View metadata, citation and similar papers at core.ac.uk

brought to you by CORE

provided by RERO DOC Digital Library

European Heart Journal (2011) **32**, 1077–1088
doi:10.1093/eurheartj/ehr076

FASTTRACK CLINICAL

Identification of a novel loss-of-function calcium channel gene mutation in short QT syndrome (SQTS6)

Christian Templin[1*†], Jelena-Rima Ghadri[2†], Jean-Sébastien Rougier[3†], Alessandra Baumer[4], Vladimir Kaplan[2], Maxime Albesa[3], Heinrich Sticht[5], Anita Rauch[4], Colleen Puleo[6], Dan Hu[6], Héctor Barajas-Martinez[6], Charles Antzelevitch[6], Thomas F. Lüscher[1,7], Hugues Abriel[3*], and Firat Duru[1,7,8]

[1]Cardiology, Cardiovascular Center, University Hospital Zurich, Raemistr. 100, 8091 Zurich, Switzerland; [2]Department of Internal Medicine, University Hospital Zurich, Zurich, Switzerland; [3]Department of Clinical Research, University of Bern, Murtenstr. 35, 3010 Bern, Switzerland; [4]Institute of Medical Genetics, University Hospital Zurich, Zurich, Switzerland; [5]Institute of Biochemistry, Friedrich-Alexander-University Erlangen-Nuernberg, Erlangen, Germany; [6]Masonic Medical Research Laboratory, Utica, NY, USA; [7]Zurich Center for Integrative Human Physiology (ZIHP), University Zurich, Zurich, Switzerland; and [8]Division of Cardiac Arrhythmia and Electrophysiology, University Hospital Zurich, Zurich, Switzerland

Received 25 November 2010; revised 21 February 2011; accepted 24 February 2011; online publish-ahead-of-print 7 March 2011

This paper was guest edited by Prof. Dr med Lars Eckardt, Cardiology and Angiology, Universitätsklinikum Münster (UKM), Germany, Email: l.eckardt@uni-muenster.de

Aims Short QT syndrome (SQTS) is a genetically determined ion-channel disorder, which may cause malignant tachyarrhythmias and sudden cardiac death. Thus far, mutations in five different genes encoding potassium and calcium channel subunits have been reported. We present, for the first time, a novel loss-of-function mutation coding for an L-type calcium channel subunit.

Methods and results The electrocardiogram of the affected member of a single family revealed a QT interval of 317 ms (QTc 329 ms) with tall, narrow, and symmetrical T-waves. Invasive electrophysiological testing showed short ventricular refractory periods and increased vulnerability to induce ventricular fibrillation. DNA screening of the patient identified no mutation in previously known SQTS genes; however, a new variant at a heterozygous state was identified in the *CACNA2D1* gene (nucleotide c.2264G > C; amino acid p.Ser755Thr), coding for the $Ca_v\alpha_2\delta$-1 subunit of the L-type calcium channel. The pathogenic role of the p.Ser755Thr variant of the *CACNA2D1* gene was analysed by using co-expression of the two other L-type calcium channel subunits, $Ca_v1.2\alpha1$ and $Ca_v\beta_{2b}$, in HEK-293 cells. Barium currents (I_{Ba}) were recorded in these cells under voltage-clamp conditions using the whole-cell configuration. Co-expression of the p.Ser755Thr $Ca_v\alpha_2\delta$-1 subunit strongly reduced the I_{Ba} by more than 70% when compared with the co-expression of the wild-type (WT) variant. Protein expression of the three subunits was verified by performing western blots of total lysates and cell membrane fractions of HEK-293 cells. The p.Ser755Thr variant of the $Ca_v\alpha_2\delta$-1 subunit was expressed at a similar level compared with the WT subunit in both fractions. Since the mutant $Ca_v\alpha_2\delta$-1 subunit did not modify the expression of the pore-forming subunit of the L-type calcium channel, $Ca_v1.2\alpha1$, it suggests that single channel biophysical properties of the L-type channel are altered by this variant.

Conclusion In the present study, we report the first pathogenic mutation in the *CACNA2D1* gene in humans, which causes a new variant of SQTS. It remains to be determined whether mutations in this gene lead to other manifestations of the J-wave syndrome.

Keywords Arrhythmia • Short QT syndrome • Novel gene mutation • Sudden cardiac death

* Corresponding authors. Tel: +41 44 255 9585, Fax: +41 44 255 4401, Email: christian.templin@usz.ch (C.T.); Tel: +41 31 632 0998, Fax: +41 31 632 0946, Email: hugues.abriel@dkf.unibe.ch (H.A.)

† These authors contributed equally to this work and are shared first authors.

Published on behalf of the European Society of Cardiology. All rights reserved. © The Author 2011. For permissions please email: journals.permissions@oup.com

Introduction

Short QT syndrome (SQTS) is a genetically determined ion-channel disorder, which may cause malignant tachyarrhythmias and sudden cardiac death (SCD). The definition of the short QT interval varies in the literature[1–5] but is generally defined as a QTc interval below 330 ms.[6,7] The diagnosis of SQTS can be made in patients with a short QTc interval who present with additional clinical findings, such as syncope, episodes of polymorphic ventricular tachycardia or ventricular fibrillation, or a family history of unexplained SCD. The disease usually affects young and healthy individuals who have no underlying structural heart disease.[2] To date, five genes have been identified that are responsible for SQTS, demonstrating a genetically heterogeneous disease (*Table 1*).[5,7–9] Short QT syndrome 1, SQTS2 and SQTS3 are caused by gain-of-function mutations of cardiac potassium channels causing hastened repolarization.[5,8,9] Short QT syndrome 1 is due to mutations in *KCNH2* encoding the α-subunit of the HERG I_{Kr} channel, which lead to heterogeneous shortening of the action potentials and refractoriness.[9] Typically, on surface electrocardiogram (ECG), the ST-segment is absent and the T-wave is tall, narrow, and symmetrical. The triggering factors are usually adrenergic-dependent; however, some cases at rest have also been described.[10] Short QT syndrome 2 is associated with mutations in *KCNQ1* encoding the α-subunit of the KvLQT1 I_{Ks} channel.[8] Short QT syndrome 3, which is caused by a mutation in *KCNJ2* is characterized by nocturnal palpitations.[5] In contrast to SQTS1, SQTS2, and SQTS3, loss-of-function missense mutations in *CACNA1C* and *CACNB2* genes, which are subunits of the cardiac L-type calcium channel, have been identified in SQTS4 and SQTS5.[7] The latter two subtypes are associated with asymmetrical T-waves, attenuated QT-heart rate relations, and the presence of atrial fibrillation. These patients may also present with a Brugada-like surface ECG pattern with or without drug provocation.[7] Loss-of-function mutations in the potassium channels have also been reported for the long QT1, long QT2, and the Andersen–Tawil syndrome (long QT7).[11–13]

Recent studies have shown that inherited cardiac arrhythmias may be caused by mutations found in the genes coding for the subunits of the L-type Ca channel.[7,14] In cardiac myocytes, $Ca_v1.2$ channels are predominant. $Ca_v1.2$ channels are formed of a pore-forming $Ca_v1.2\alpha1$ subunit (*CACNA1C* gene), which carries the main biophysical and pharmacological properties of the channels, and accessory subunits $Ca_v\beta_{2b}$ (*CACNB2b* gene) and $Ca_v\alpha_2\delta$-1 (*CACNA2D1* gene). $Ca_v\beta$ and $Ca_v\alpha_2\delta$ subunits play a dual role in regulating both the biophysical properties and trafficking of Ca_v channels.[15,16] $Ca_v\gamma$ subunits are also expressed in cardiac myocytes; however, there is no evidence that they interact with cardiac $Ca_v1.2$ channels.[17]

In this study, mutation analysis was performed for all genes, which have been identified to be linked to SQTS (*KCNH2*, *KCNQ1*, *KCNJ2*, *CACNA1C*, and *CACNB2b*) and in those that are considered to be candidate genes for SQTS (*CACNA2D1*, *KCNJ8*, and *Sur2A*).[7,14] We report a new variant of SQTS caused by a mutation in the gene encoding the $Ca_v\alpha_2\delta$-1 subunit of the L-type calcium channel (*CACNA2D1*).

Table 1 Update of the currently known genes causing short QT syndrome and their mutations

SQTS type	Gene symbol	Ionic current	Effect of mutation on channel function	Reference
SQTS1	*KCNH2*	I_{Kr}	↑	Brugada *et al.*[9]
SQTS2	*KCNQ1*	I_{Ks}	↑	Bellocq *et al.*[8]
SQTS3	*KCNJ2*	I_{K1}	↑	Priori *et al.*[5]
SQTS4	*CACNA1C*	I_{Ca}	↓	Antzelevitch *et al.*[7]
SQTS5	*CACNB2b*	I_{Ca}	↓	Antzelevitch *et al.*[7]

I_{Kr}, rectifier K^+ current rapid component; I_{Ks}, rectifier K^+ current slow component; I_{K1}, inward rectifier K^+ current; I_{Ca}, Ca^{2+} current.

Methods

Molecular genetic analysis

Genomic DNA from the index patient was extracted from peripheral blood leucocytes using a commercial kit (Gentra System, Puregene, Valencia, CA, USA). All exons and intron borders of cardiac ion channel genes including but not limited to all isoforms of *KCNQ1*, *KCNH2*, *SUR2A*, *KCNJ8*, *KCNJ2*, *CACNA1C*, *CACNB2b*, and *CACNA2D1* genes were amplified and analysed by direct sequencing from both directions using an ABI PRISM 3100-Avant Automatic DNA sequencer (Applied Biosystems, Foster City, CA, USA). Genomic DNA from 410 reference alleles from healthy ethnically matched controls from the USA and 402 ethnically matched healthy reference alleles from southern Germany were used as controls. The *CACNA2D1* primers used for screening are shown in *Table 2*. Family screening of the c.2264G > C (p.Ser755Thr) mutation in *CACNA2D1* was performed according to standard protocols after exon amplification by polymerase chain reaction (PCR) with the intronic primers: forward 5′-GGGGGAGAGCA GATAGTAGC-3′ and reverse 5′-GCTATGCTGATGCATTGCT-3′. The 352 bp PCR products were directly sequenced on both strands in the family and on one strand in the controls using an ABI 3730 capillary sequencer. The reference sequence was based on ENSE00002087663. Written informed consent was obtained from all family members prior to the genetic study.

cDNA constructs

Rabbit $Ca_v1.2\alpha1$ (cP15381.1), $Ca_v\beta_{2b}$ (P54288), and $Ca_v\alpha_2\delta$-1 (P13806) cDNAs, inserted into pCARDHE, pBH17, and pCA1S, respectively, were gifts from Dr G.S. Pitt (Division of Cardiology, Department of Medicine, Duke University Medical Center, Durham, NC, USA). CD8 cDNAs subcloned into EBOpcD-Leu2 [American Type Culture Collection (*ATCC*), Rockville, MD, USA]. *CACNA2D1* mutation was engineered into wild-type (WT) cDNA using the QuickChange Kit (Stratagene, USA) and verified by sequencing.

Transfections

For electrophysiology experiments, HEK-293 cells were transiently transfected using the calcium phosphate method and 0.3 μg cDNAs of each Ca_v channel subunit ($Ca_v1.2\alpha1$, $Ca_v\beta_{2b}$, and $Ca_v\alpha_2\delta$-1; ratio 1:1:1) together with 1.0 μg of empty $pcDNA_{3.1}$ vector. In addition, 0.5 μg of cDNA encoding CD8 antigen was added to all transfections

Table 2 Primers of *CACNA2D1* gene

CACNA2D1 gene segment	Primers sequence (5′ → 3′)	
Exon	**Sense**	**Anti-sense**
1	5′-GTGTGCTGCTCTTCCTCCG-3′	5′-CGCGACTCGGGAACCGAC-3′
2	5′-GACATAGTCGGTGCTAGGAG-3′	5′-GTTCACAGTACCTAGCAGTAC-3′
3	5′-CAGGGTGGTGTTTCTAATCAG-3′	5′-GATGAACACAGTTACTAAGAAG-3′
4	5′-CTGATGATGGCAGAGGTAAC-3′	5′-GGCTAACTTAATTGGCCCTG-3′
5	5′-CAATGCAAGATGTAATATCACTG-3′	5′-CTCATGCAGTCTAACATTGTC-3′
6	5′-GTGAGTGCTAATACCTGAATG-3′	5′-CATGGATGCAGGCTGTCCT-3′
7	5′-GATCCAGTCAAACTGTCCTC-3′	5′-CAGTTTAAAGTGACTGTGGTC-3′
8	5′-GAACATTGAAGTACGTAAGTGA-3′	5′-CATTACCCACTTGAACTCATC-3′
9	5′-CATTGTCTACTTAGATAGAAGTG-3′	5′-GTCTTGATATGGCTTCATTGC-3′
10	5′-GTACACATACTGATATTGGGAG-3′	5′-CAGGTCAGTAAGATAGTCTTG-3′
11	5′-GAGTAAGCAATGCAATACCGT-3′	5′-CTTCTGCCTGCACACATCTG-3′
12	5′-GATCCAGGAACCAGTTCTTAG-3′	5′-GCATGAGTTGCTTGTGAATATG-3′
13	5′-CTGAAGGCTTTACTGGCCTC-3′	5′-CATGTTCAGAATCTTACTCTTG-3′
14	5′-GCCTGTGTGTTTGTTGTGAAG-3′	5′-CAATGTATCAACAAGATACTCAG-3′
15	5′-CCATACCACCTATGGAGTAC-3′	5′-CAATGAAGGGATCAAGTAGAC-3′
16	5′-CTTCAGTAGGTGCCTAGTAG-3′	5′-GTGGTTATCGCATAGGCAGC-3′
17	5′-GACACTGAGAGTGCTTCACC-3′	5′-GTTCCTTTGCTAAGATAACTG-3′
18	5′-CTTGGCACTTAGGTAATTCTC-3′	5′-GTTGCAGCTAAATTGGTAACAG-3′
19	5′-GCAGTATCAAATACAGCACTC-3′	5′-CCGTTCAACAGATACTTGTAG-3′
20	5′-GAGAACAACTACAGATACTGG-3′	5′-CATCAAGAAACCTAAAGCAATAG-3′
21	5′-GATCATACCTTTGTAAAGATGAG-3′	5′-CATGTTGGGAACTTTTCTAGTG-3′
22	5′-GACTCTGGATGGCAAGACTG-3′	5′-CCTGCTCATATTCTATCCATG-3′
23	5′-CCTCAGACTACAGCTGTAC-3′	5′-CTAAGTTTTGAGTGATCAAG-3′
24	5′-GTACCATGTTATGAAGTTATCC-3′	5′-GATTCCATAATGTGATATGAAAC-3′
25	5′-GAAGTAACAAGAAGCTCAATAG-3′	5′-CGTATCCTATGATATACTATAACC-3′
26	5′-CTACTAAATCCATTCATTTCCTG-3′	5′-GTAATAGCAGACATTAGTACT-3′
27	5′-GAGATGTCTTCCTTAAACATCC-3′	5′-CAATGTAATCTAATGGCAATCAG-3′
28	5′-CTGATGCATTGCTCAGTAATG-3′	5′-CTGATGCATTGCTCAGTAATG-3′
29	5′-CAGTTAGCCTAGTGTATACAAC-3′	5′-CAACTTCAGAGGTAACTAGTC-3′
30	5′-CAGGTTGTGGCTAATGAATAC-3′	5′-GAATTCTACTTCAGTGTAGTGG-3′
31	5′-CAAGGTTATAACATGCAATGCT-3′	5′-CAGTTGAGACCGAAGAGAAC-3′
32	5′-CATGTATATAATGGGGTAAAGAC-3′	5′-CTTAGCATGCATTTCTTAATGG-3′
33	5′-GCTCCTCAGTTGTACTTCAG-3′	5′-GTAATATGTCTGCTACTGATGG-3′
34	5′-GACATCGCTCAGCATATGTG-3′	5′-GGAAGACTCTAAAGAGGCTG-3′
35	5′-CACTTGACTCTGAACAAGATC-3′	5′-CAAGATGGCTATGAGATCAGG-3′
36	5′-CACAGTAGTAAACAAGCCAG-3′	5′-CTCACATCTCTGACTCCAAC-3′
37	5′-CTCCTATTGTGCTGGGAATG-3′	5′-CGAGGTGATCAGAGCAGTC-3′
38	5′-GTGTTGGATGAGAGTAATGATG-3′	5′-GAAGCAACTGTCAAGTTTATGC-3′
39	5′-GCATTTGTCAAATGATGCTAGG-3′	5′-GACATGCAGCCAGTGGGTG-3′

as a reporter gene. At 24 h post-transfection, cells were split at low density (3% of one 25 cm^2 flask per dish). Anti-CD8 beads (Dynal®, Oslo, Norway) were used to identify transfected cells. For biochemistry experiments, 10 cm dishes of HEK-293 cells were transfected using lipofectamine LTX® (Invitrogen, Basel, Switzerland) according to the manufacturer's instructions. Cells were used 48 h after transfection. The ratio cDNAs/lipofectamine was 7.5 μg cDNAs/30 μL Lipofectamine. The ratio of the different constructs was similar to those used in patch-clamp experiments.[16]

Electrophysiology

Whole-cell currents were measured at room temperature (22–23°C) using a VE-2 amplifier (Alembic Instrument, USA). The internal pipette solution was composed of (in mmol/L) 60 CsCl, 70 Cs-aspartate, 1 $MgCl_2$, 10 HEPES, 11 EGTA, and 5 Mg-ATP, pH 7.2, with CsOH. The external solution contained (in mmol/L) 130 NaCl, 5.6 KCl, 5 $BaCl_2$, 1 $MgCl_2$, 10 HEPES, and 11 D-glucose, pH 7.4, with NaOH. Data were analysed using pClamp software, version 10.2 (Axon Instruments, Union City, CA, USA). Barium current densities (pA/pF) were

calculated dividing the peak current by the cell capacitance. Activation curves and steady-state inactivation curves were fitted with the following single Boltzmann's equation: $y = 1/\{1 + \exp[(V_h - V_{50})/k]\}$, in which y is the normalized conductance or peak current at a given holding potential (V_h), V_{50} the voltage at which half of the channels are activated ($V_{50,act}$) or inactivated ($V_{50,inact}$), respectively, and k the slope factor.

Western blots

Ten centimetre HEK-293 cell dishes were lysed in 1.0 mL of lysis buffer (50 mmol/L HEPES, pH 7.4, 150 mmol/L NaCl, 10% glycerol, 1% Triton, and 1 mmol/L EGTA supplemented with protease inhibitors). Protein concentration was systematically determined by performing a Bradford assay (Coo protein dosage kit; Interchim, Montluçon, France). Seventy micrograms of proteins were loaded on SDS–

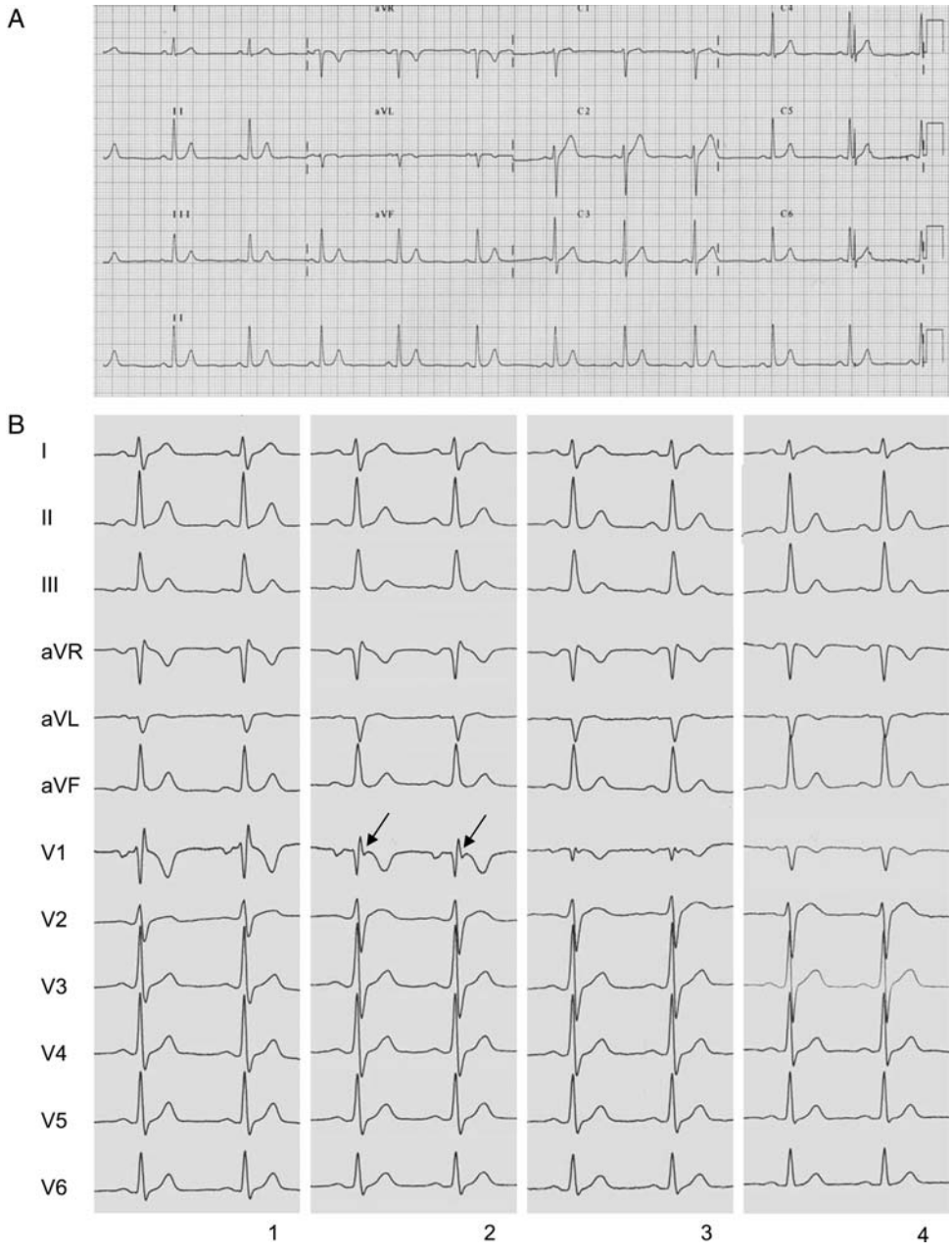

Figure 1 Twelve-lead electrocardiogram of the patient with short QT syndrome. (*A*) QT interval is 317 ms (QTc 329 ms) on resting surface electrocardiogram at presentation (paper speed 25 mm/s). (*B*) Surface electrocardiogram prior to and after flecainide challenge test. (1) Twelve-lead electrocardiogram shows incomplete right bundle branch block at baseline. (2) Ten minutes after flecainide (2 mg/kg) administration, a prominent notch in V1 in the early ST-segment (arrow) is depicted. Notably, the ST-segment becomes more convex. (3) Fifteen minutes after flecainide challenge, reduction in the QRS amplitude in V1 is observed. (4) Twenty minutes later, a prominent Q-wave is seen in V1. Six hours later, the right precordial electrocardiogram changes returned to baseline.

PAGE gel. Protein transfer was done with the dry system transfer i-blot® from Invitrogen. Immunoblotting was done using the snap-id® system of Millipore (Zug, Switzerland). Fluorescent secondary antibodies at dilution 1/10 000 were used and detection was realized using the LICOR system® (Lincoln, NE, USA).

Cell membrane biotinylation

Cells were treated for 30 min at 4°C with 4 mL biotin per 10 cm dish (1 mg/mL; EZ link Sulfo-NHS-SS-Biotin; Pierce, Rockford, IL, USA), washed three times with cold PBS 1× containing 200 mmol/L glycine and lysed with 1 mL/dish of lysis buffer. Fifty microlitres of streptavidin sepharose beads (GE Healthcare Europe, Glattbrugg, Switzerland) were added to 1 mg of HEK-293 cell lysate and incubated 2 h on a wheel at 4°C. The beads were washed five times with lysis buffer and resuspended in sample buffer (Invitrogen). Eluted proteins were analysed by western blot.

Antibodies

Antibodies against $Ca_v1.2\alpha1$ (ACC003) (Alomone, Jerusalem, Israel), $Ca_v\beta_{2b}$ (ab54920), and $Ca_v\alpha_2\delta$-1 (ab2864) (Abcam, Cambridge, UK) were used at a dilution of 1/200 for $Ca_v1.2\alpha1$ and $Ca_v\beta_{2b}$ and 1/1000 for $Ca_v\alpha_2\delta$-1. Monoclonal antibodies raised against actin were purchased from Sigma-Aldrich (Sigma-Aldrich Chemie, Buchs, Switzerland) and used at a dilution of 1/1000.

Computational analysis of the p.Ser755Thr mutation in *CACNA2D1*

The domain architecture of *CACNA2D1* was deduced from the BioInfoBank MetaServer.[18] Transmembrane regions were identified using Memsat 3.[19,20] The structure of the sensory domain of *CACNA2D1* was modelled with Modeler 6.2 using the crystal structure of Histidine Kinase Dctb Sensor Domain as a template (PDB code 3by9). The Ser755Thr mutation was generated using Sybyl 7.3 (Tripos Inc.), and DS Visualizer v2.5 (Accelrys Inc.) was used for structure analysis and visualization.

Statistical analysis

Data are presented as means ± SEM. Unpaired, two-tailed Student's *t*-test was used to compare the means; $P < 0.05$ was considered significant.

Results

Clinical case

An otherwise healthy, 17-year-old female of Caucasian origin had a sudden loss of consciousness while sitting during a church service. Basic life support was administered immediately and the initial rhythm recorded ventricular fibrillation which was successfully terminated in a stable sinus rhythm after two external defibrillation shocks. The patient was subsequently transferred to a hospital by emergency medical personnel. The ECG revealed a QT interval of 317 ms (QTc 329 ms) with tall, narrow, and symmetrical T-waves, suggestive of SQTS (*Figure 1A*). Transthoracic echocardiography excluded any structural heart disease and coronary angiography showed normal coronary arteries. Invasive electrophysiological testing revealed AH and HV intervals within the normal range; the atrial effective refractory period was 180 ms and AV block cycle length was 420 ms. There was an AH jump of 70 ms, suggesting the presence of a slow pathway. Programmed stimulation from the high right atrium induced a non-sustained atrial tachycardia originating from the posterior left atrium, as well as atrial fibrillation, which terminated spontaneously. Programmed stimulation from the right ventricular apex with S1/S2 of 600/260 ms could induce a polymorphic ventricular tachycardia

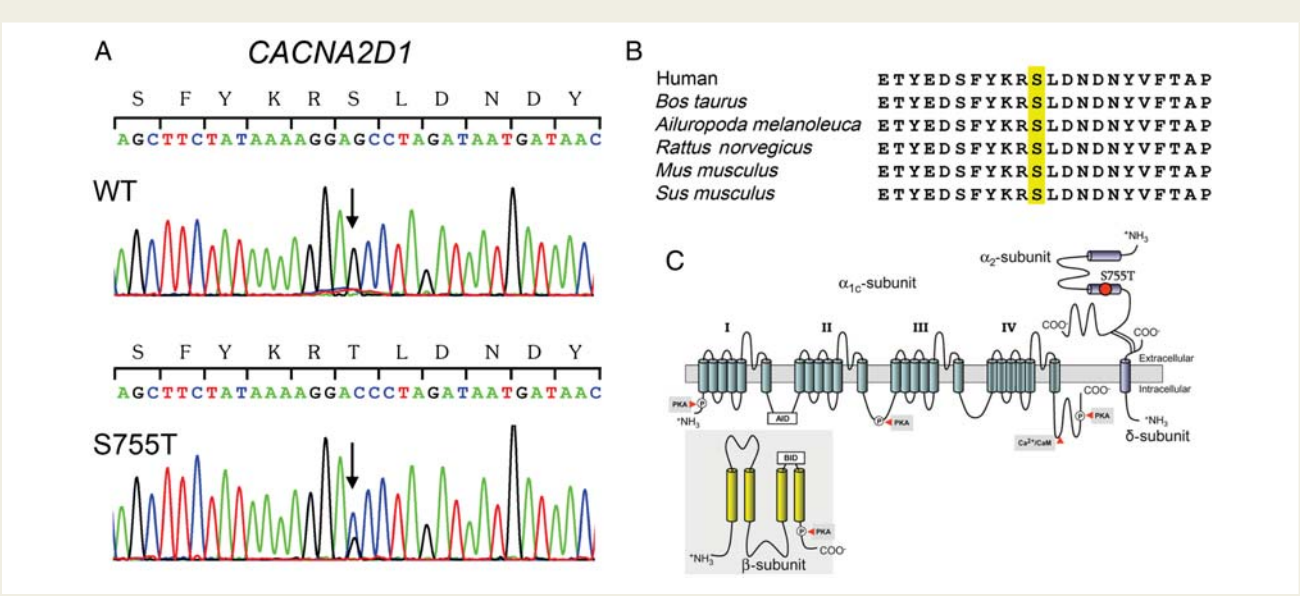

Figure 2 Genetic analysis identified a novel *CACNA2D1* mutation. (*A*) Electropherograms of wild-type (WT) and mutant *CACNA2D1* gene showing a heterozygous transition c.2264G > C predicting replacement of serine by threonine at position 755 (p.Ser755Thr). (*B*) Amino acid sequence alignment showing that serine at position 755 is highly conserved among mammalian species. (*C*) Predicted topology of the L-type calcium channel $Ca_v\alpha_2\delta$-1 subunit showing the location of the S755T mutation (red circle) at the external carboxyl terminal of *CACNA2D1*. AID, α-subunit-interacting domain. BID, β-subunit-interacting domain.

degenerating into ventricular fibrillation, which was terminated externally. An incomplete right bundle branch block was observed intermittently. Flecainide provocation (2 mg/kg) did not reveal a typical Brugada ECG pattern, despite placement of the right precordial leads in a superior position. However, distinct repolarization changes in V1 were observed (*Figure 1B*). The patient was treated with a β-blocker (nebivolol, 5 mg q.d.) and she underwent implantation of a single-chamber implantable cardioverter defibrillator (ICD). At 24-month follow-up, the patient has not reported any symptomatic arrhythmias and the

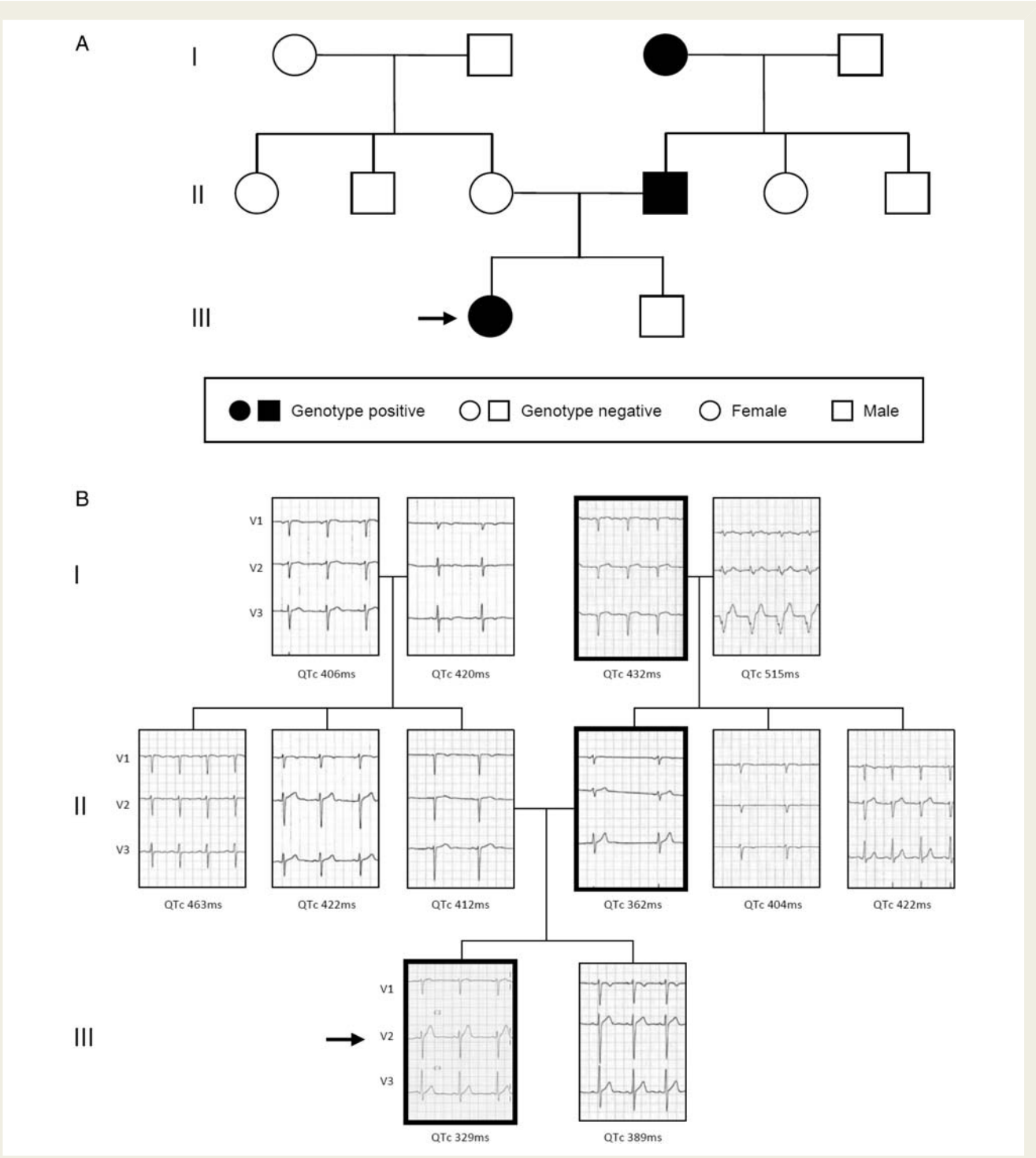

Figure 3 (*A*) Pedigree of the reported family. (*B*) Right precordial electrocardiographic leads (V1, V2, and V3; 25 mm/s; electrodes were placed in the normal position) and the QTc intervals of the family members. Paternal grandmother had a previous anteroseptal myocardial infarction and paternal grandfather had an implanted pacemaker. The black arrows mark the index patient.

ICD registered only one episode of a non-sustained ventricular tachycardia (five beats with a cycle length of 250 ms).

Molecular genetics analysis

Screening of the genomic DNA of the patient has identified no mutations in previously known SQTS genes, i.e. *KCNH2*, *KCNQ1*, *KCNJ2*, *CACNA1C*, and *CACNB2b*. In addition, no mutations in *KCNJ8* and *SUR2* have been detected. A novel heterozygous mutation consisting of a G-to-C transition at nucleotide 2264 (c.2264 G > C) in *CACNA2D1* predicting a substitution of a threonine for serine at residue 755 (p.Ser755Thr) of *CACNA2D1* ($Ca_v\alpha_2\delta$-1) subunit of the cardiac L-type calcium channel (Ser755Thr) was found (*Figure 2A*). The mutation was not found in 812 reference alleles from healthy ethnically matched controls. Alignment of the amino acid sequence of $Ca_v\alpha_2\delta$-1 indicates that serine at position 755 is highly conserved among species (*Figure 2B*). Residue Ser755 is located at the external carboxyl terminal region of $Ca_v\alpha_2$ (*Figure 2C*).

Family screening showed that the father who had borderline QTc interval and the paternal grandmother were also carriers of this variant (*Figure 3*). Both mutation carriers were asymptomatic regarding syncope, seizures, or arrhythmic events. In addition, no prior SCD event or arrhythmia has occurred in this family before. Baseline ECG of both family members did not display a Brugada syndrome (BrS) pattern. Electrophysiological and drug challenge testing to the affected family members was recommended; however, this was declined.

Functional analyses

In order to determine a possible pathogenic role of the p.Ser755Thr variant in the *CACNA2D1* gene, *in vitro* analyses were performed using co-expression of the two other L-type calcium channel subunits, $Ca_v1.2\alpha1$ and $Ca_v\beta_{2b}$, in HEK-293 cells. First, protein expression of the three subunits was verified by performing western blots of total lysates of HEK-293 cells. The p.Ser755Thr variant of the $Ca_v\alpha_2\delta$-1 subunit was expressed at a similar level compared with the WT subunit (*Figure 4A*). In addition, this variant did not modify the expression of the pore-forming subunit of the L-type Ca channel, $Ca_v1.2\alpha1$. Secondly, barium currents (I_{Ba}) were recorded in these cells under voltage-clamp conditions using the whole-cell configuration. Co-expression of the p.Ser755Thr $Ca_v\alpha_2\delta$-1 subunit strongly reduced I_{Ba} by more than 70% when compared with the co-expression of the WT variant (*Figure 4B* and *C*, and *Table 3*). Small positive shifts of the inactivation and activation curves were observed when the mutant $Ca_v\alpha_2\delta$-1 subunit was expressed (*Figure 4D*). These alterations of the biophysical properties of the current are similar to the condition in which the L-type channel is expressed without the $Ca_v\alpha_2\delta$ subunit (*Figure 4E* and *F*, and *Table 3*). Then, in order to understand the mechanisms underlying the strong reduction in I_{Ba} caused by the co-expression of $Ca_v\alpha_2\delta$-1 p.Ser755Thr, we analysed the expression of $Ca_v1.2\alpha1$ and $Ca_v\alpha_2\delta$-1 subunits at the cell surface by performing membrane protein biotinylation assays. As shown in *Figure 5*, the mutant variant of the $Ca_v\alpha_2\delta$-1 subunit was equally well expressed at the cell surface when compared with the WT control. A similar result was obtained for the $Ca_v1.2\alpha1$. Altogether these results suggest that the mutation p.Ser755Thr of $Ca_v\alpha_2\delta$-1 alters some of the single channel biophysical properties of the L-type channel at the cell membrane.

Computational analyses

CACNA2D1 is predicted to be anchored in the cellular membrane by a carboxy-terminal transmembrane helix (residues 1067–1087). The largest part of the protein, including the site of the p.Ser755Thr mutation, is located in the extracellular space. A computational analysis based on sequence and structure similarities suggests that the mutation is located in a sensory domain (residues 659–889) whose exact physiological function is not known to date. Molecular modelling of this domain reveals that Ser755 is located at a sterically demanding position and is oriented towards the interior of a protein (*Figure 6A*). In the WT protein, Ser755 tightly packs against a valine (Val799) of the opposite β-strand (*Figure 6B*). The additional methyl group present in Thr755 of the mutant protein cannot be accommodated in the core of the protein and leads to clashes with the side chain of Val799 (*Figure 6C*). These clashes may potentially alter some of the, yet unknown, functions of this protein.

Discussion

In the present study, we report a variant in the *CACNA2D1* gene (c.2264G > C; p.Ser755Thr), which, on the basis of our functional studies, is most likely pathogenic. Mutations in *CACNA2D1* hence cause a new variant of SQTS. This gene has been recently proposed to be linked to BrS and early repolarization syndrome;[21] however, the pathogenicity of the found variants has, thus far, not been demonstrated. In the present report, the patient who presented with survived SCD in the absence of structural heart disease presented a short QTc interval at baseline and repolarization abnormalities in the right precordial leads during flecainide challenge. Invasive electrophysiological testing in this patient showed short atrial refractory periods and induction of non-sustained atrial tachycardia and atrial fibrillation during programmed stimulation in the atrium and polymorphic ventricular tachycardia and ventricular fibrillation during programmed stimulation in the ventricle. The *CACNA2D1* mutation most likely plays a role in the occurrence of these electrophysiological findings and in the observed intermittent incomplete right bundle branch block. Repolarization abnormalities that may be suggestive of BrS were neither present at rest nor during flecainide provocation test. Likewise, the patient did not show an early repolarization pattern on numerous baseline and follow-up ECGs as well as during drug challenge. Recently, BrS and early repolarization syndrome, both associated with J-wave abnormalities, were proposed to represent different manifestations of a 'J-wave syndrome'.[22] Although the genetic origin of early repolarization syndrome is still unknown, mutations in α and β calcium channel subunits lead to a clinical phenotype very close to BrS.[7,14] Hence, based on the observation that the $Ca_v\alpha_2\delta$-1 subunit mutation lead to a decreased calcium current (similarly to the α and β mutations) and that a peculiar alteration of the J-wave was observed upon flecainide challenge, it may be suggested that these clinical manifestations including a prominent shortening of the QT interval are

also part of a continuum caused by decreased calcium current. It remains to be seen whether, in the future, more patients with similar phenotypes caused by mutations in calcium channel genes will permit a better definition of this J-wave syndrome.

Genetic analyses revealed that both father and paternal grandmother were heterozygous carriers of the missense mutation p.Ser755Thr in *CACNA2D1*. However, both carriers failed to display any ECG alteration compatible with SQTS. This observation is in line with the fact that penetrance and expressivity in patients with SQTS are known to be very variable, ranging from asymptomatic carriers to symptomatic patients with atrial-, ventricular fibrillation, and SCD.[23] Compared with the congenital long QT syndrome 1–3, robust genotype–phenotype correlations are still lacking for SQTS. This is the reason why Brugada *et al.*[24] have proposed that management must still rely on clinical findings.

The mutation that has been found in the *CACNA2D1* gene affects the L-type calcium channel, which is responsible for the cardiac

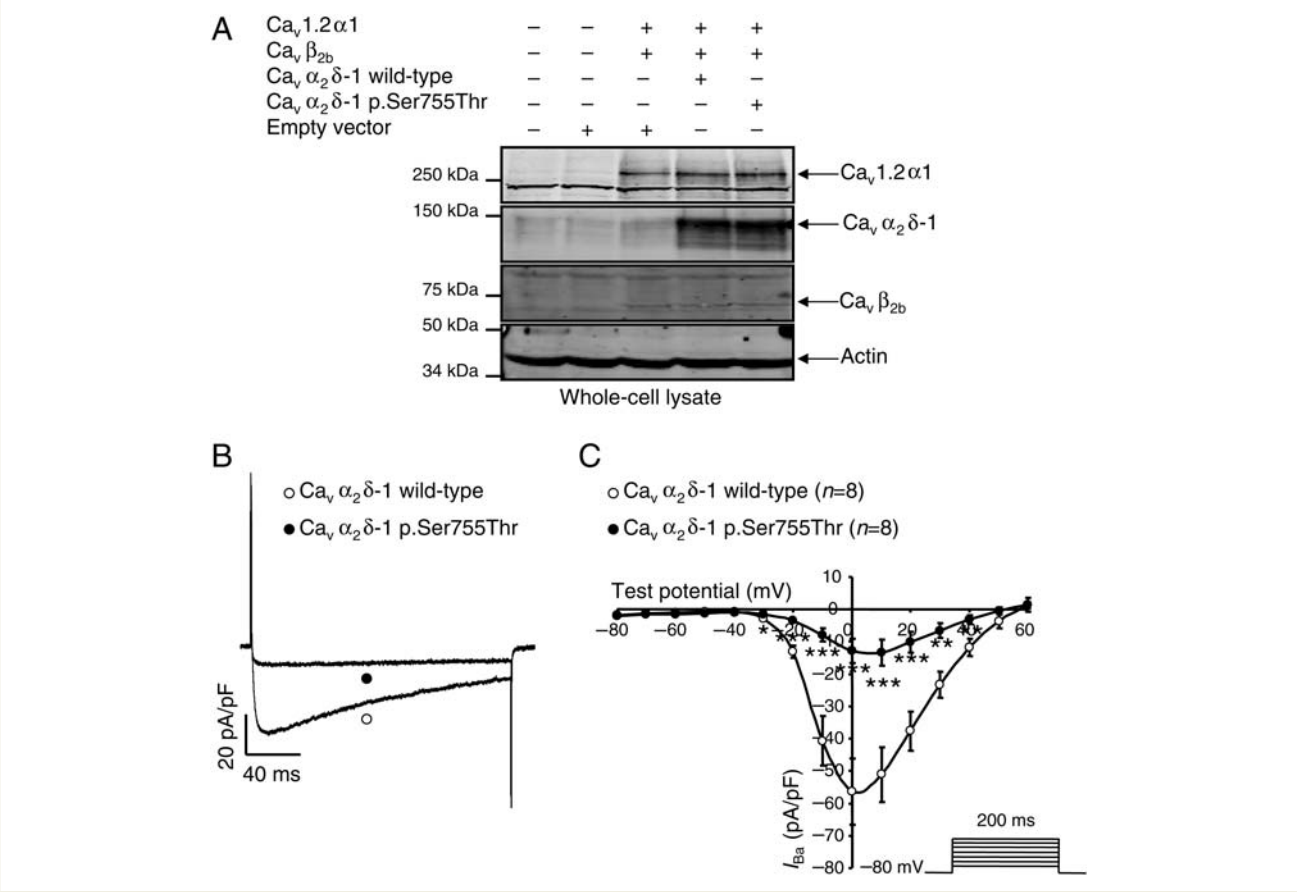

Figure 4 The barium current (I_{Ba}) is reduced by $Ca_v\alpha_2\delta$-1 p.Ser755Thr. (*A*) Western blot showing that the expression of all subunits is not modified in the condition where $Ca_v\alpha_2\delta$-1 p.Ser755Thr is expressed compared with the control condition ($Ca_v1.2\alpha1/Ca_v\beta_{2b}/Ca_v\alpha_2\delta$-1). (*B*) Representative whole-cell current traces at 0 mV during 200 ms. (*C*) *I–V* relationships recorded (protocol in inset) from HEK-293 cells transfected with $Ca_v1.2\alpha1/Ca_v\beta_{2b}/Ca_v\alpha_2\delta$-1 channels (open circle) or with $Ca_v1.2\alpha1/Ca_v\beta_{2b}/Ca_v\alpha_2\delta$-1 p.Ser755Thr (filled circle). (*D*) Activation curves and steady-state inactivation curves recorded (protocol in inset) from HEK-293 cells transfected under the same condition of transfection as in (*C*) and fitted as mentioned in the Methods section. Activation curves: $Ca_v1.2\alpha1/Ca_v\beta_{2b}/Ca_v\alpha_2\delta$-1 (open circle) $V_{1/2} = -10.5 \pm 0.6$ mV, $K = 5.9 \pm 0.4$; $Ca_v1.2\alpha1/Ca_v\beta_{2b}/Ca_v\alpha_2\delta$-1 p.Ser755Thr (filled circle) $V_{1/2} = -8.4 \pm 0.9$ mV (*compared with $Ca_v1.2\alpha1/Ca_v\beta_{2b}/Ca_v\alpha_2\delta$-1), $K = 6.1 \pm 0.3$ (n.s. compared with $Ca_v1.2\alpha1/Ca_v\beta_{2b}/Ca_v\alpha_2\delta$-1). Steady-state inactivation curves: $Ca_v1.2\alpha1/Ca_v\beta_{2b}/Ca_v\alpha_2\delta$-1 (open diamond) $V_{1/2} = -33.1 \pm 0.9$ mV, $K = 7.9 \pm 0.3$; $Ca_v1.2\alpha1/Ca_v\beta_{2b}/Ca_v\alpha_2\delta$-1 p.Ser755Thr (filled diamond) $V_{1/2} = -30.6 \pm 0.5$ mV (**compared with $Ca_v1.2\alpha1/Ca_v\beta_{2b}/Ca_v\alpha_2\delta$-1), $K = 8.2 \pm 0.5$ (n.s. compared with $Ca_v1.2\alpha1/Ca_v\beta_{2b}/Ca_v\alpha_2\delta$-1). (*E*) *I–V* relationships recorded (protocol in inset) from HEK-293 cells transfected with $Ca_v1.2\alpha1/Ca_v\beta_{2b}/Ca_v\alpha_2\delta$-1 channels (open circle) or with $Ca_v1.2\alpha1/Ca_v\beta_{2b}$ (filled circle). (*F*) Activation curves and steady-state inactivation curves recorded (protocol in inset) from HEK-293 cells transfected in the same condition as in (*E*) and fitted as mentioned in the Methods section. Activation curves: $Ca_v1.2\alpha1/Ca_v\beta_{2b}/Ca_v\alpha_2\delta$-1 (open circle) $V_{1/2} = -10.5 \pm 0.6$ mV, $K = 5.9 \pm 0.4$; $Ca_v1.2\alpha1/Ca_v\beta_{2b}$ (filled circle) $V_{1/2} = -2.0 \pm 0.6$ mV (***compared with $Ca_v1.2\alpha1/Ca_v\beta_{2b}/Ca_v\alpha_2\delta$-1), $K = 7.6 \pm 0.3$ (**compared with $Ca_v1.2\alpha1/Ca_v\beta_{2b}/Ca_v\alpha_2\delta$-1). Steady-state inactivation curves: $Ca_v1.2\alpha1/Ca_v\beta_{2b}/Ca_v\alpha_2\delta$-1 (open diamond) $V_{1/2} = -33.1 \pm 0.9$ mV, $K = 7.9 \pm 0.3$; $Ca_v1.2\alpha1/Ca_v\beta_{2b}$ (filled diamond) $V_{1/2} = -26.0 \pm 2.8$ mV (*compared with $Ca_v1.2\alpha1/Ca_v\beta_{2b}/Ca_v\alpha_2\delta$-1), $K = 12.4 \pm 1.3$ (**compared with $Ca_v1.2\alpha1/Ca_v\beta_{2b}/Ca_v\alpha_2\delta$-1). The number of cells recorded is indicated in parentheses. *$P < 0.05$, **$P < 0.01$, and ***$P < 0.001$.

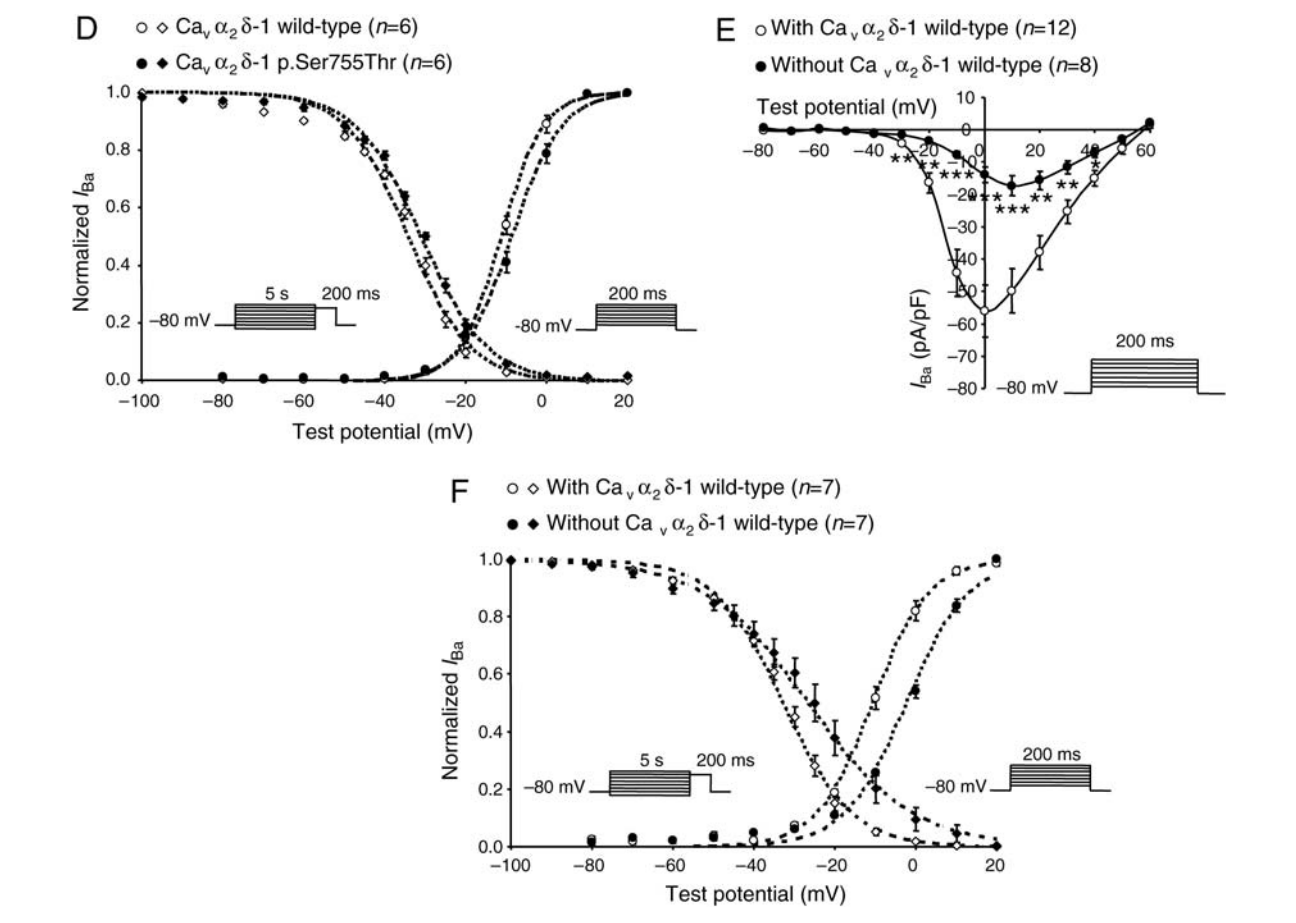

Figure 4 *Continued.*

Table 3 Effect of $Ca_v\alpha_2\delta$-1 wild-type and $Ca_v\alpha_2\delta$-1 p.Ser755Thr on Ca_v voltage dependence of activation and steady-state inactivation

	$Ca_v1.2\alpha1/Ca_v\beta_{2b}$	$Ca_v1.2\alpha1/Ca_v\beta_{2b}/Ca_v\alpha_2\delta$-1	$Ca_v1.2\alpha1/Ca_v\beta_{2b}/Ca_v\alpha_2\delta$-1 p.Ser755Thr
Activation			
$V_{50,act}$ (mV)	−2.0 ± 0.6 (7)***	−10.5 ± 0.6 (13)$^{\#}$	−8.4 ± 0.9 (6)
k (mV)	7.6 ± 0.3 (7)**	5.9 ± 0.4 (13) n.s.	6.1 ± 0.3 (6)
Steady-state inactivation			
$V_{50,inact}$ (mV)	−26.0 ± 2.8 (7) n.s.	−33.1 ± 0.9 (13)$^{\#\#}$	−30.6 ± 0.5 (6)
k (mV)	12.4 ± 1.3 (7)**	7.9 ± 0.3 (13) n.s.	8.2 ± 0.5 (6)
Current density (pA/pF)			
Peak (pA/pF and %)	17 ± 3 (10) n.s. 30 ± 5% n.s.	56 ± 9 (20)$^{\#\#\#}$ 100 ± 16%$^{\#\#\#}$	13 ± 4 (8) 23 ± 7%

$Ca_v1.2\alpha1/Ca_v\beta_{2b}$ channels were expressed without $Ca_v\alpha_2\delta$ with $Ca_v\alpha_2\delta$-1 wild-type or $Ca_v\alpha_2\delta$-1 p.Ser755Thr. V_{50} values indicates the respective voltage at which 50% of the channels are activated ($V_{50,act}$) or inactivated ($V_{50,inact}$), and k the slopes of the corresponding Boltzmann-fitted curves described in the Methods section. Amplitude of current is expressed in current densities and percentage of variation (%) from the controls ($Ca_v1.2\alpha1/Ca_v\beta_{2b}/Ca_v\alpha_2\delta$-1; 100%). Values are means ± SEM. The number of cells is indicated in parentheses. n.s., not significant compared with $Ca_v1.2\alpha1/Ca_v\beta_{2b}/Ca_v\alpha_2\delta$-1 p.Ser755Thr condition.

**$P < 0.01$.

***$P < 0.001$.

$^{\#}P < 0.05$.

$^{\#\#}P < 0.01$.

$^{\#\#\#}P < 0.001$.

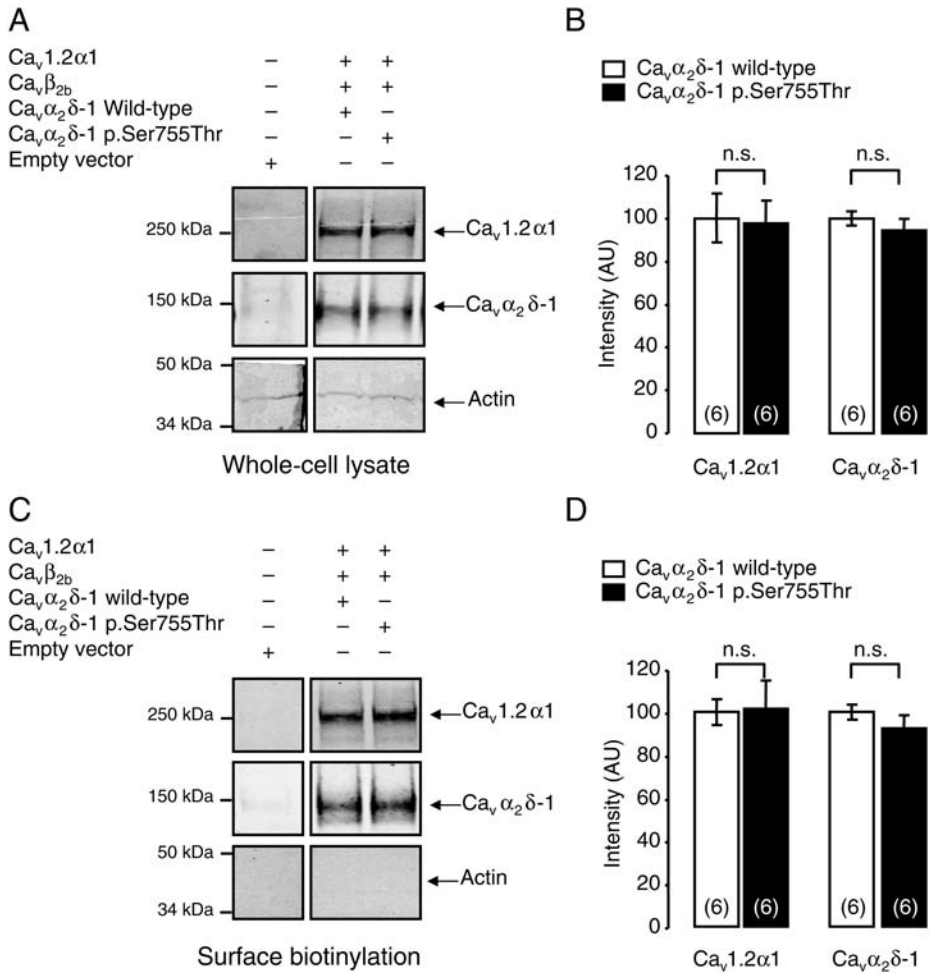

Figure 5 Surface biotinylation assays were performed using $Ca_v1.2\alpha1/Ca_v\beta_{2b}/Ca_v\alpha_2\delta$-1 and $Ca_v1.2\alpha1/Ca_v\beta_{2b}/Ca_v\alpha_2\delta$-1 p.Ser755Thr subunit-transfected HEK-293 cells. (*A*) Western blots showing $Ca_v1.2\alpha1$ and $Ca_v\alpha_2\delta$-1 subunits detected in the whole-cell lysates and (*C*) corresponding biotinylated fraction. (*B* and *D*) Bar graphs summarizing the effect of the mutation on the expression of $Ca_v1.2\alpha1$ and $Ca_v\alpha_2\delta$-1 subunits in whole-cell lysates (*B*) and in biotinylated fractions (*D*). The number of independent experiments is indicated in parentheses; n.s., not significant compared with control cells transfected with $Ca_v1.2\alpha1/Ca_v\beta_{2b}/Ca_v\alpha_2\delta$-1 subunits.

action potential plateau phase and the cytoplasmic Ca^{2+} transients regulating the contraction force.[25,26] The auxiliary $Ca_v\alpha_2\delta$-1 subunit is known to be involved in the forward trafficking, membrane turnover, and modulation of biophysical properties of the pore-forming $Ca_v\alpha1$ subunits.[27] The molecular mechanisms underlying these effects are however only poorly understood. Until now, no demonstrated pathogenic variants in the $Ca_v\alpha_2\delta$-1 subunit have been associated with SQTS. The variant carried by the patient is most likely the cause of the SQTS phenotype since it strongly reduces the $Ca_v\alpha1$-mediated current in the used cellular expression system. The fact that the cellular protein expression of the three expressed subunits in the cell lysates and of the $Ca_v\alpha1$ at the cell membrane was not found to be modified by the mutant $Ca_v\alpha_2\delta$-1 subunit suggests that this variant alters some of the biophysical single channel properties of channel at the membrane. Further experiments are needed to understand this intriguing finding.

Interestingly, it has been shown that loss-of-function mutations in *CACNA1C*, the gene encoding the pore-forming subunit of the cardiac Ca^{2+} current, contribute to SQTS type 4, whereas gain-of-function mutations produce non-inactivating Ca^{2+} currents and prolonged action potentials leading to a prolonged QT interval on the ECG defined as the Timothy syndrome or congenital long QT syndrome type 8.[28,29] Similarly, gain- or loss-of-function mutations found in the genes coding for Na^+ or K^+ channels were found to be responsible for either long QT and BrS phenotypes. It may therefore be speculated that gain- or loss-of-function mutations in the *CACNA2D1* gene could also lead to different arrhythmogenic phenotypes. On the basis of the results of the present study and the recent work of Burashnikov *et al.*,[14] BrS and SQTS may be allelic disorders caused by loss-of-function mutations in *CACNA2D1*. Obviously, further work is needed to understand the detailed mechanisms underlying the molecular mechanisms of these clinical entities.

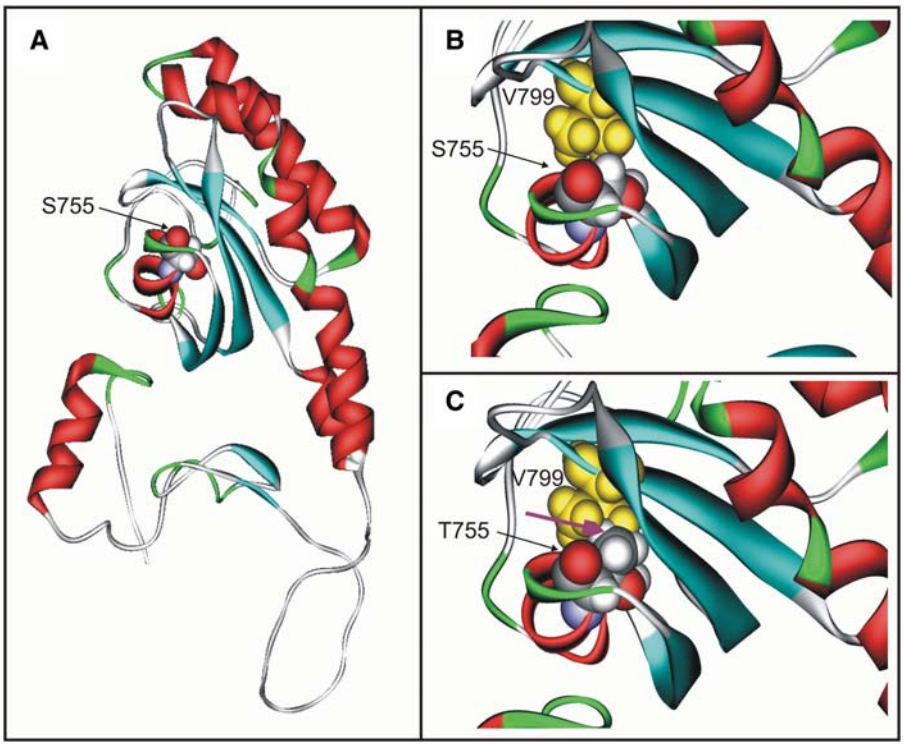

Figure 6 Model of the sensory domain (residues 659–889) of *CACNA2D1*. (*A*) Helices, sheets, turns, and coil regions are coloured in red, cyan, green, and white, respectively. (*B* and *C*) The site of the p.Ser755Thr mutation is shown in space-filled presentation and is shown as an enlargement in the right panels. (*B*) Interactions of Ser755 and Val799 in the WT protein. The hydrophobic moieties of both side chains pack tightly, but no clashes are observed. Residue 755 is coloured by atom type and Val799 is depicted in yellow. (*C*) Interactions of Thr755 and Val799 in the mutant protein. The magenta arrow indicates clashes between the methyl groups of Thr755 and Val799. Colour coding as in (*B*).

In summary, this study identifies for the first time a pathogenic variant in the *CACNA2D1* gene, encoding the $Ca_v\alpha_2\delta$-1 subunit of the L-type calcium channel, as cause of SQTS, hence defining SQTS6. These findings underline the crucial role of the different subunits of the cardiac L-type calcium channel in inherited channelopathies in general, and in SQTS in particular. Whether mutations in *CACNA2D1* may cause other manifestations of J-wave syndrome[22] remains to be investigated.

Acknowledgements

We are grateful to Ulrike Hüffmeier, MD, Institute of Human Genetics, Friedrich-Alexander-University of Erlangen-Nuernberg, Germany, for the allocation of control samples. We thank the index patient and family for participating in this study.

Funding

C.T. is supported by a grant of the Swiss National Science Foundation 'Sonderprogramm Universitäre Medizin' (No. 33CM30-124112/1). The group of H.A. is supported by the University of Bern and the Swiss National Science Foundation grant 310030_120707. F.D. is supported by the Foundation for Cardiovascular Research, Zurich, Switzerland. The work was further supported by the Zurich Center of Integrated Human Physiology. C.A. is supported by grant HL47678 (CA) from NHLBI of the National Institutes of Health and by New York State and Florida Free and Accepted Masons.

Conflict of interest: none declared.

References

1. Gaita F, Giustetto C, Bianchi F, Wolpert C, Schimpf R, Riccardi R, Grossi S, Richiardi E, Borggrefe M. Short QT syndrome: a familial cause of sudden death. *Circulation* 2003;**108**:965–970.
2. Gussak I, Brugada P, Brugada J, Wright RS, Kopecky SL, Chaitman BR, Bjerregaard P. Idiopathic short QT interval: a new clinical syndrome? *Cardiology* 2000;**94**:99–102.
3. Schimpf R, Wolpert C, Bianchi F, Giustetto C, Gaita F, Bauersfeld U, Borggrefe M. Congenital short QT syndrome and implantable cardioverter defibrillator treatment: inherent risk for inappropriate shock delivery. *J Cardiovasc Electrophysiol* 2003;**14**:1273–1277.
4. Schulze-Bahr E, Breithardt G. Short QT interval and short QT syndromes. *J Cardiovasc Electrophysiol* 2005;**16**:397–398.
5. Priori SG, Pandit SV, Rivolta I, Berenfeld O, Ronchetti E, Dhamoon A, Napolitano C, Anumonwo J, di Barletta MR, Gudapakkam S, Bosi G, Stramba-Badiale M, Jalife J. A novel form of short QT syndrome (SQT3) is caused by a mutation in the KCNJ2 gene. *Circ Res* 2005;**96**:800–807.
6. Patel C, Yan GX, Antzelevitch C. Short QT syndrome: from bench to bedside. *Circ Arrhythm Electrophysiol* 2010;**3**:401–408.
7. Antzelevitch C, Pollevick GD, Cordeiro JM, Casis O, Sanguinetti MC, Aizawa Y, Guerchicoff A, Pfeiffer R, Oliva A, Wollnik B, Gelber P, Bonaros EP Jr, Burashnikov E, Wu Y, Sargent JD, Schickel S, Oberheiden R, Bhatia A, Hsu LF, Haissaguerre M, Schimpf R, Borggrefe M, Wolpert C. Loss-of-function mutations in the cardiac calcium channel underlie a new clinical entity characterized by ST-segment elevation, short QT intervals, and sudden cardiac death. *Circulation* 2007;**115**:442–449.

8. Bellocq C, van Ginneken AC, Bezzina CR, Alders M, Escande D, Mannens MM, Baro I, Wilde AA. Mutation in the KCNQ1 gene leading to the short QT-interval syndrome. *Circulation* 2004;**109**:2394–2397.
9. Brugada R, Hong K, Dumaine R, Cordeiro J, Gaita F, Borggrefe M, Menendez TM, Brugada J, Pollevick GD, Wolpert C, Burashnikov E, Matsuo K, Wu YS, Guerchicoff A, Bianchi F, Giustetto C, Schimpf R, Brugada P, Antzelevitch C. Sudden death associated with short-QT syndrome linked to mutations in HERG. *Circulation* 2004;**109**:30–35.
10. Giustetto C, Di Monte F, Wolpert C, Borggrefe M, Schimpf R, Sbragia P, Leone G, Maury P, Anttonen O, Haissaguerre M, Gaita F. Short QT syndrome: clinical findings and diagnostic-therapeutic implications. *Eur Heart J* 2006;**27**:2440–2447.
11. Sanguinetti MC, Curran ME, Zou A, Shen J, Spector PS, Atkinson DL, Keating MT. Coassembly of K(V)LQT1 and minK (IsK) proteins to form cardiac I(Ks) potassium channel. *Nature* 1996;**384**:80–83.
12. Curran ME, Splawski I, Timothy KW, Vincent GM, Green ED, Keating MT. A molecular basis for cardiac arrhythmia: HERG mutations cause long QT syndrome. *Cell* 1995;**80**:795–803.
13. Plaster NM, Tawil R, Tristani-Firouzi M, Canun S, Bendahhou S, Tsunoda A, Donaldson MR, Iannaccone ST, Brunt E, Barohn R, Clark J, Deymeer F, George AL Jr, Fish FA, Hahn A, Nitu A, Ozdemir C, Serdaroglu P, Subramony SH, Wolfe G, Fu YH, Ptacek LJ. Mutations in Kir2.1 cause the developmental and episodic electrical phenotypes of Andersen's syndrome. *Cell* 2001; **105**:511–519.
14. Burashnikov E, Pfeiffer R, Barajas-Martinez H, Delpon E, Hu D, Desai M, Borggrefe M, Haissaguerre M, Kanter R, Pollevick GD, Guerchicoff A, Laino R, Marieb M, Nademanee K, Nam GB, Robles R, Schimpf R, Stapleton DD, Viskin S, Winters S, Wolpert C, Zimmern S, Veltmann C, Antzelevitch C. Mutations in the cardiac L-type calcium channel associated with inherited J-wave syndromes and sudden cardiac death. *Heart Rhythm* 2010;**7**:1872–1882.
15. Viard P, Butcher AJ, Halet G, Davies A, Nurnberg B, Heblich F, Dolphin AC. PI3K promotes voltage-dependent calcium channel trafficking to the plasma membrane. *Nat Neurosci* 2004;**7**:939–946.
16. Dolphin AC. Assembly and targeting of voltage-dependent calcium channels. In: Moss SJ, Henley J, eds. *Receptor and Ion Channel Trafficking*. Oxford: Oxford University Press; 2002. p58–86.
17. Hansen JP, Chen RS, Larsen JK, Chu PJ, Janes DM, Weis KE, Best PM. Calcium channel gamma6 subunits are unique modulators of low voltage-activated (Cav3.1) calcium current. *J Mol Cell Cardiol* 2004;**37**:1147–1158.
18. Ginalski K, Elofsson A, Fischer D, Rychlewski L. 3D-Jury: a simple approach to improve protein structure predictions. *Bioinformatics* 2003;**19**:1015–1018.
19. Jones DT, Taylor WR, Thornton JM. A model recognition approach to the prediction of all-helical membrane protein structure and topology. *Biochemistry* 1994;**33**:3038–3049.
20. von Heijne G. Membrane protein structure prediction. Hydrophobicity analysis and the positive-inside rule. *J Mol Biol* 1992;**225**:487–494.
21. Burashnikov E, Pfeiffer R, Barajas-Martinez H, Delpon E, Hu D, Desai M, Borggrefe M, Haissaguerre M, Kanter R, Pollevick GD, Guerchicoff A, Laino R, Marieb M, Nademanee K, Nam GB, Robles R, Schimpf R, Stapleton DH, Viskin S, Winters S, Wolpert C, Zimmern S, Veltmann C, Antzelevitch C. Mutations in the cardiac L-type calcium channel associated with inherited J-wave syndromes and sudden cardiac death. *Heart Rhythm* 2010;**7**:1872–1882.
22. Antzelevitch C, Yan GX. J wave syndromes. *Heart Rhythm* 2010;**7**:549–558.
23. Patel U, Pavri BB. Short QT syndrome: a review. *Cardiol Rev* 2009;**17**:300–303.
24. Brugada R, Hong K, Cordeiro JM, Dumaine R. Short QT syndrome. *CMAJ* 2005; **173**:1349–1354.
25. Berridge MJ, Bootman MD, Lipp P. Calcium—a life and death signal. *Nature* 1998; **395**:645–648.
26. Catterall WA. Structure and regulation of voltage-gated Ca^{2+} channels. *Annu Rev Cell Dev Biol* 2000;**16**:521–555.
27. Bauer CS, Tran-Van-Minh A, Kadurin I, Dolphin AC. A new look at calcium channel alpha(2)delta subunits. *Curr Opin Neurobiol* 2010;**20**:563–571.
28. Splawski I, Timothy KW, Decher N, Kumar P, Sachse FB, Beggs AH, Sanguinetti MC, Keating MT. Severe arrhythmia disorder caused by cardiac L-type calcium channel mutations. *Proc Natl Acad Sci USA* 2005;**102**:8089–8096; discussion 8086–8088.
29. Splawski I, Timothy KW, Sharpe LM, Decher N, Kumar P, Bloise R, Napolitano C, Schwartz PJ, Joseph RM, Condouris K, Tager-Flusberg H, Priori SG, Sanguinetti MC, Keating MT. Ca(V)1.2 calcium channel dysfunction causes a multisystem disorder including arrhythmia and autism. *Cell* 2004;**119**:19–31.